

Effects of Interactions on the Critical Temperature of a Trapped Bose Gas

Robert P. Smith, Robert L. D. Campbell, Naaman Tammuz, and Zoran Hadzibabic

Cavendish Laboratory, University of Cambridge, J. J. Thomson Avenue, Cambridge CB3 0HE, United Kingdom

(Received 5 April 2011; published 23 June 2011)

We perform high-precision measurements of the condensation temperature of a harmonically trapped atomic Bose gas with widely tunable interactions. For weak interactions we observe a negative shift of the critical temperature in excellent agreement with mean-field theory. However for sufficiently strong interactions we clearly observe an additional positive shift, characteristic of beyond-mean-field critical correlations. We also discuss nonequilibrium effects on the apparent critical temperature for both very weak and very strong interactions.

DOI: 10.1103/PhysRevLett.106.250403

PACS numbers: 03.75.Hh, 03.75.Kk, 67.85.-d

The effect of interparticle interactions on the Bose-Einstein condensation temperature of a dilute gas has been theoretically debated for more than 50 years, since the pioneering work of Lee and Yang [1]. In a uniform system there is no interaction shift of the critical temperature T_c at the level of mean-field theory. However, consideration of the correlations between particles which develop near the critical point leads to the conclusion that repulsive interactions *enhance* condensation, i.e., shift T_c above the ideal gas value T_c^0 [2–6].

Ultracold atomic gases offer an excellent testbed for fundamental theories of many-body physics [7,8]. However, in these systems the problem of the interaction shift of T_c is even more complex because they are harmonically confined. In this case, at least for weak interactions, the T_c shift is dominated by an opposing mean-field effect, which reduces the critical temperature [9]. Within experimental precision, previous measurements [10–12] were consistent with the mean-field theory and could not discern the effects of critical correlations.

In this Letter, we report on high-precision measurements of the T_c shift in a potassium (^{39}K) gas with tunable interactions [13,14]. We employ a Feshbach resonance [15] to extend the previously explored range of interaction strengths and eliminate several key sources of statistical and systematic errors. This allows us to clearly reveal the long-sought beyond-mean-field effects on the critical temperature. We also examine the stringent requirements for equilibrium T_c measurements, which are violated in the regimes of either very weak or very strong interactions. In nonequilibrium gases we observe evidence for “superheated” condensates which survive at an apparent temperature above the equilibrium T_c , suggesting that strong dissipation can stabilize the coherent condensed state.

Historically, most theoretical work focused on a uniform gas, and for several decades there was no consensus on the functional form, or even on the sign of the T_c shift (see, e.g., [4,6]). It is now generally believed that the shift is positive and to leading order given by [4,5]

$$\frac{\Delta T_c}{T_c^0} \approx 1.3an^{1/3} \approx 1.8 \frac{a}{\lambda_0}, \quad (1)$$

where $\Delta T_c = T_c - T_c^0$, $a > 0$ is the s -wave scattering length, n the particle density, and λ_0 the thermal wavelength at T_c^0 . The positive ΔT_c implies condensation at a phase space density below the ideal gas critical value of $n\lambda^3 = \zeta(3/2) \approx 2.612$ (where ζ is the Riemann function).

For a harmonically trapped gas, T_c is defined for a given atom number N , rather than for a given density n . For an ideal gas, $k_B T_c^0 = \hbar \bar{\omega} [N/\zeta(3)]^{1/3}$, where $\bar{\omega}$ is the geometric mean of the trapping frequencies and $\zeta(3) \approx 1.202$. This corresponds to a phase space density in the trap center equal to the uniform system critical value, $n(0)\lambda^3 = \zeta(3/2)$. The interaction shift of the critical point can be expressed either as $\Delta T_c(N)$ (for comparison with theoretical literature) or as $\Delta N_c(T)$ (for easier visualization, as in Figs. 1 and 2).

The two opposing effects of repulsive interactions on the critical point of a trapped gas are illustrated in Fig. 1, where we sketch the density distribution at the condensation point for an ideal (dotted blue line) and an interacting (solid red line) gas at the same temperature. In the spirit of the local

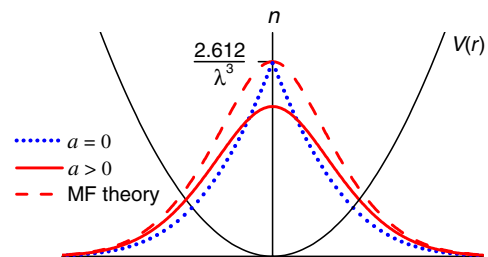


FIG. 1 (color online). Opposing effects of interactions on the critical point of a Bose gas in a harmonic potential $V(r)$. Compared to an ideal gas (dotted blue line) with the same T_c , repulsive interactions reduce the critical density, but also broaden the density distribution (solid red line). Mean-field theory (dashed line) captures only the latter effect, and predicts an increase of the critical atom number N_c at fixed temperature T , equivalent to a decrease of T_c at fixed N .

density approximation, the critical density should be reduced by repulsive interactions. However, interactions also broaden the density distribution. For weak interactions the latter effect is dominant, making the overall interaction shift $\Delta N_c(T)$ positive, or equivalently $\Delta T_c(N)$ negative.

The negative T_c shift due to the broadening of the density distribution in a harmonically trapped gas can be calculated using mean-field (MF) theory, which neglects the reduction of the critical phase space density implied by Eq. (1) (see dashed line in Fig. 1). This approach gives [9]

$$\frac{\Delta T_c}{T_c^0} \approx -3.426 \frac{a}{\lambda_0}. \quad (2)$$

The dominance of the negative MF shift of T_c over the positive beyond-MF one goes beyond the difference in numerical prefactors in Eqs. (2) and (1). At the condensation point, in a nonuniform system only the central region of the cloud is close to criticality, which reduces the net effect of critical correlations so that they are expected to affect T_c only at a higher order in a/λ_0 . The MF result of Eq. (2) should therefore be exact at first order in a/λ_0 . Despite several attempts to theoretically combine the effects of MF repulsion and beyond-MF correlations on T_c for a harmonically trapped gas [16–20], no consensus has been reached beyond the expectation that the additional beyond-MF shift should be positive.

Previous measurements [10–12], consistent with Eq. (2), were performed for a/λ_0 ranging from 0.007 [12] to 0.024 [11]. We explore the range $0.001 < a/\lambda_0 < 0.06$, using the 402.5 G Feshbach resonance in the $|F, m_F\rangle = |1, 1\rangle$ state of ^{39}K [21]. As in [14,22], we produce ^{39}K condensates in a crossed optical dipole trap which provides a close to isotropic trapping potential, with $\bar{\omega}/2\pi = 75\text{--}85$ Hz for the measurements reported here.

To measure the critical point we prepare a partially condensed cloud, fix the optical trap depth, and let the atom number decay towards N_c through inelastic processes; meanwhile, elastic collisions redistribute particles between condensed and thermal components, and the temperature remains essentially constant [23]. We prepare clouds with various condensed fractions at $a = 135a_0$, where a_0 is the Bohr radius. We then adjust a to the desired value by ramping the Feshbach field, and wait for an a -dependent hold time t_{hold} before releasing the gas from the trap and measuring its momentum distribution through absorption imaging after 19 ms of time-of-flight (TOF). In the last part of the Letter we discuss the strict requirements on the relationship between t_{hold} , the elastic scattering rate γ_{el} , and the relevant atom-number decay time τ for the measurements of T_c to faithfully reflect equilibrium properties of the gas. For now we focus on the measurements which we trust to be in equilibrium.

In addition to extending the a/λ_0 range, the Feshbach resonance provides two experimental advantages essential for the precision and accuracy of our measurements:

(i) For each measurement series at a given a and λ_0 , we concurrently take a reference measurement with a different

a , same $\bar{\omega}$ and very similar N , hence very similar λ_0 . Specifically, for the reference point we choose a small a such that $a/\lambda_0 \approx 0.005$. We thus directly access the small T_c shift due to the difference in a/λ_0 , and essentially eliminate all a -independent systematic errors that usually affect absolute measurements of $T_c(N, \bar{\omega}, a)$. These include uncertainties in the absolute calibration of N and $\bar{\omega}$, as well as the additional T_c shifts due to finite-size effects [7] and the small trap anharmonicity [14].

(ii) We home in on the critical point by turning off the interactions during TOF. To do this we quickly (in ≤ 2 ms) ramp the Feshbach field to 350 G immediately after the release of the gas from the trap. This minimizes the expansion of small condensates and allows us to reliably detect condensed fractions as small as $\sim 10^{-3}$ (see Fig. 2).

Figure 2 illustrates our differential measurement. Here $a = 274a_0$, $\lambda_0 \approx 10^4 a_0$, and $a = 56a_0$ for the reference series. If the two series had identical N_c values, we could directly read off the differential $\Delta T_c(N)$. To correct for the small (few %) difference in N_c we apply the ideal gas scaling, $T_c \propto N^{1/3}$, to the reference series. The second-order error in ΔT_c due to the small ($< 2\%$) T_c shift at $a/\lambda_0 \approx 0.005$ is much smaller than our statistical error bars. For visual clarity, in Fig. 2 we instead scale to the same temperature and display $\Delta N_c(T)$.

In Figs. 2(b) and 2(c) we show the relationship between the condensed (N_0) and thermal (N') atom number near the critical point [24]. The rise of N_0 in Fig. 2(b) is not simply vertical because the thermal component in a partially condensed gas is not saturated at N_c [22]; one can also see that this effect is more pronounced at higher a . It is therefore essential to carefully extrapolate N' to the $N_0 = 0$ limit in

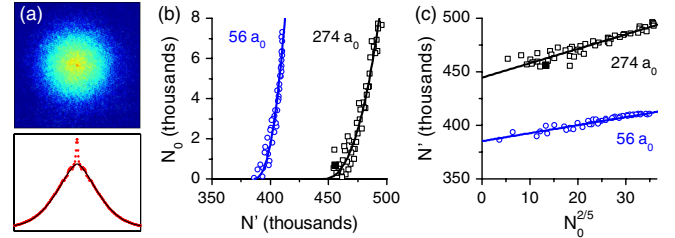


FIG. 2 (color online). Determination of the critical point and differential interaction shift. (a) An absorption image of a cloud with 450 000 atoms and a 0.14% condensed fraction. We show an azimuthally averaged cut through the column density for illustrative purposes, while the full 2D distribution is used for fitting. The gas was prepared at a large scattering length, $a = 274a_0$, but the interactions were turned off in TOF. (b) Condensed (N_0) versus thermal (N') atom number for two concurrently taken series with $a = 56a_0$ (blue circles) and $a = 274a_0$ (black squares). Note that all points correspond to condensed fractions below 2%. The data are scaled to the same temperature ($T = 240$ nK) and show the shift of the critical point in the form $\Delta N_c(T)$. The solid point corresponds to the image shown in (a). Solid lines show the extrapolation to $N_0 = 0$, necessary to accurately determine N_c . (c) N' is plotted versus $N_0^{2/5}$ for the same data as in (b), showing more clearly the extrapolation procedure.

order to accurately determine N_c . We extrapolate using $N' = N_c + S_0 N_0^{2/5}$, with the nonsaturation slope $S_0(T, \bar{\omega}, a)$ calculated with no free parameters following [22].

In Fig. 3 we summarize our equilibrium measurements of the interaction shift $\Delta T_c/T_c^0$. We took data with $N \approx (2-8) \times 10^5$ (corresponding to $T_c^0 \approx 180-330$ nK) in order to verify that our results depend only on the interaction parameter a/λ_0 . The MF result of Eq. (2) fits the data very well for $a/\lambda_0 \lesssim 0.01$. For larger a/λ_0 we observe a clear deviation from this prediction. All data points are fitted well by a second-order polynomial, $\Delta T_c/T_c^0 = b_1(a/\lambda_0) + b_2(a/\lambda_0)^2$, with $b_1 = -3.5 \pm 0.3$ and $b_2 = 46 \pm 5$ [25]. Logarithmic corrections to this functional form are predicted (see, e.g., [18]), but are not discernible within our error bars.

The value of b_1 is in excellent agreement with the MF prediction of -3.426 [9]. The value of b_2 strongly excludes zero, and its sign is consistent with the expected effect of beyond-MF correlations. These measurements provide the first observation of beyond-MF effects on the transition temperature of a harmonically trapped gas.

To conclude this part of the Letter, we assess our systematic errors. In general, interactions increase the kinetic energy of thermal atoms during TOF, resulting in an a -dependent error in T which does not cancel out in our differential measurements. This error is minimized by fitting the high-energy wings of the thermal distribution (excluding the central thermal radius) [26]. We also turn the interactions off at the beginning of TOF, but the reduction of a is gradual over ≈ 2 ms. We measure the difference between (apparent) T with interactions “on” and “off” during TOF to be approximately linear in a/λ_0 , and about 4% for $a = 400a_0$ and $\lambda_0 \approx 10^4 a_0$. By varying the time at which we turn off a , we estimate our residual error to be 1%–2% at $a/\lambda_0 = 0.04$. This estimate is supported by numerical simulations. Additionally, interactions modify the in-trap momentum distribution. This *reduces* the

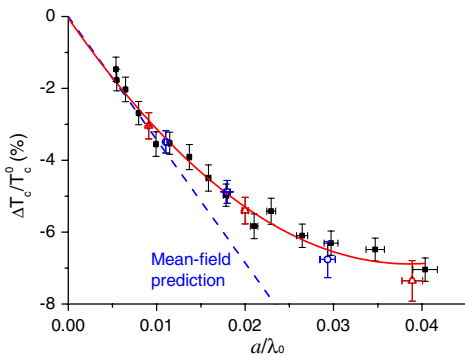


FIG. 3 (color online). Interaction shift of T_c . Data points were taken with $N \approx 2 \times 10^5$ (blue circles), 4×10^5 (black squares), and 8×10^5 (red triangles) atoms. The dashed line is the mean-field result $\Delta T_c/T_c^0 = -3.426a/\lambda_0$. The solid line shows a second-order polynomial fit to the data (see text). Vertical error bars show statistical errors. Horizontal error bars reflect the 0.1 G uncertainty in the position of the Feshbach resonance.

apparent T because the positive chemical potential preferentially enhances population of low-energy states. We numerically estimate this effect to also be approximately linear in a/λ_0 , and about -2% at $a/\lambda_0 = 0.04$. Fortunately, the two effects partially cancel, resulting in a net error in $\Delta T_c/T_c^0$ of at most $\pm 1\%$ at $a/\lambda_0 = 0.04$.

In the rest of the Letter we discuss the equilibrium conditions required for our measurements, and the non-equilibrium effects revealed when they are violated.

In general, a system with continuous dissipation can only be “close to” thermodynamic equilibrium. For an atomic gas, the proximity to equilibrium depends on the dimensionless parameter $\gamma_{el}\tau$, which measures the relative rates of elastic and inelastic processes. In practice the γ_{el} required for equilibrium measurements also depends on the measurement precision. We measure N_c to about 1%, so we require that the gas continuously (re-)equilibrates on a time scale τ corresponding to only 1% atom-loss. We thus require about 100 times higher γ_{el} than one would naively conclude by taking the $1/e$ lifetime of the cloud as the relevant time scale. Equilibration is usually considered to take about 3 collisions per particle [27]; for all measurements shown in Fig. 3 we made sure that $\gamma_{el}\tau > 5$. All of our data also satisfy the condition $t_{\text{hold}} > \tau > 1/\bar{\omega}$, necessary for global equilibrium to be established.

An interesting question in its own right is what happens if we violate these stringent equilibrium criteria. In Fig. 4(a) we show measurements with $N \approx 4 \times 10^5$ atoms ($\lambda_0 \approx 10^4 a_0$), extending beyond the equilibrium region shown in Fig. 3. We still show only measurements satisfying $t_{\text{hold}} > \tau > 1/\bar{\omega}$ and $\gamma_{el}t_{\text{hold}} > 5$, so that there is nominally enough time for global equilibrium to be

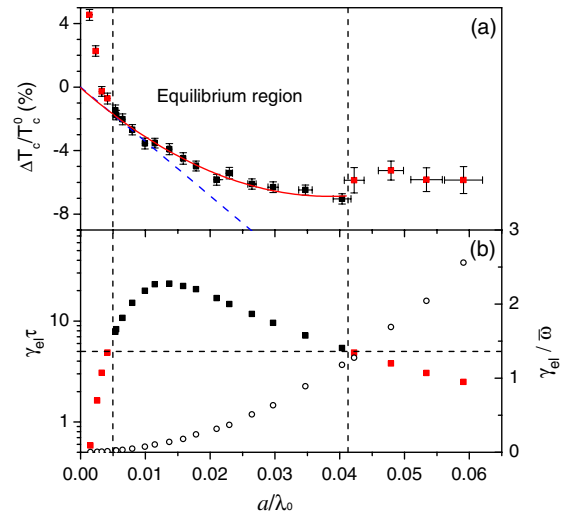


FIG. 4 (color online). Nonequilibrium effects. (a) $\Delta T_c/T_c^0$ for $N \approx 4 \times 10^5$ atoms is determined following the procedure which assumes equilibrium. At both low and high a the apparent T_c deviates from the equilibrium curve. (b) Equilibrium criteria (see text): $\gamma_{el}\tau$ (solid squares) is the number of elastic collisions per particle during 1% atom loss; $\gamma_{el}/\bar{\omega} = 1$ (open circles) marks the onset of the hydrodynamic regime.

established. However if $\gamma_{\text{el}}\tau$ is too small, the elastic collisions cannot “keep up” with the continuously present dissipation. The resulting nonequilibrium effects can thus not be eliminated by simply extending t_{hold} , but are an intrinsic property of the system. In Fig. 4(b) we plot $\gamma_{\text{el}}\tau$, based on calculated γ_{el} [28] and τ measured near the critical point. Individually, $\gamma_{\text{el}} \approx 0.7\text{--}1000\text{ s}^{-1}$ and $\tau \approx 2\text{ ms--}1\text{ s}$ vary vastly as a function of a (γ_{el} increasing and τ decreasing), but the breakdown of equilibrium occurs at very similar values of $\gamma_{\text{el}}\tau$ in the low- and high- a limit.

Nonequilibrium phenomena necessarily depend on additional factors such as the initial conditions, so we do not expect our quantitative results to be universal and discuss only qualitative trends.

In the small- a limit we observe a smooth rapid rise of the apparent T_c above the equilibrium curve (and hence above T_c^0 for $a \rightarrow 0$). We can qualitatively understand this effect within a simple picture. In this regime, losses are most likely dominated by one-body processes which equally affect N_0 and N' . The net effect of equilibrating elastic collisions would therefore be to transfer atoms from the condensate to the thermal cloud. However the dissipation rate is too high compared to γ_{el} , and so N_0 remains nonzero even after the total atom number drops below the equilibrium critical value N_c (i.e. the measured T_c is above the equilibrium value). Note that strictly speaking T is not defined out of equilibrium, but the absolute value of the observed effect is sufficiently small that an equilibrium distribution function fits the data very well and provides a good measure of the energy content of the cloud.

Our measurements in the large- a limit suggest that the initial breakdown of equilibrium again results in condensates surviving above the equilibrium T_c . However the physics in this regime is much richer, with several potentially competing effects requiring further investigation. For example, three-body decay affects N_0 and N' differently, the thermal component is far from saturation [22], and the gas also enters the hydrodynamic regime, $\gamma_{\text{el}}/\bar{\omega} > 1$ [see Fig. 4(b)].

In conclusion, we have performed high-precision studies of the effects of interactions on Bose-Einstein condensation of a trapped atomic gas. In the regime where equilibrium measurements are possible, our most important observation is the clear deviation from mean-field behavior for sufficiently strong interactions. The additional positive shift of the critical temperature is a clear signature of the condensation-enhancing effect of critical fluctuations. These measurements should provide motivation and guidance for further theoretical studies of this difficult problem. We also studied nonequilibrium condensation phenomena, for both very weak and very strong interactions. Further study of these effects should prove useful for understanding condensation in intrinsically out-of-equilibrium systems, such as polariton gases.

We thank M. Holzmann, J. Dalibard, and M. Köhl for useful discussions. This work was supported by EPSRC (Grant No. EP/I010580/1) and the Newton Trust.

- [1] T.D. Lee and C.N. Yang, *Phys. Rev.* **105**, 1119 (1957); **112**, 1419 (1958).
- [2] M. Bijlsma and H.T.C. Stoof, *Phys. Rev. A* **54**, 5085 (1996); G. Baym *et al.*, *Phys. Rev. Lett.* **83**, 1703 (1999); M. Holzmann and W. Krauth, *Phys. Rev. Lett.* **83**, 2687 (1999); M. Holzmann, G. Baym, J.-P. Blaizot, and F. Laloë, *Phys. Rev. Lett.* **87**, 120403 (2001); H. Kleinert, *Mod. Phys. Lett. B* **17**, 1011 (2003).
- [3] J.D. Reppy *et al.*, *Phys. Rev. Lett.* **84**, 2060 (2000).
- [4] P. Arnold and G. Moore, *Phys. Rev. Lett.* **87**, 120401 (2001).
- [5] V.A. Kashurnikov, N.V. Prokof'ev, and B.V. Svistunov, *Phys. Rev. Lett.* **87**, 120402 (2001).
- [6] G. Baym *et al.*, *Eur. Phys. J. B* **24**, 107 (2001); J.O. Andersen, *Rev. Mod. Phys.* **76**, 599 (2004); M. Holzmann *et al.*, *C.R. Physique* **5**, 21 (2004).
- [7] F. Dalfovo, S. Giorgini, L.P. Pitaevskii, and S. Stringari, *Rev. Mod. Phys.* **71**, 463 (1999).
- [8] I. Bloch, J. Dalibard, and W. Zwerger, *Rev. Mod. Phys.* **80**, 885 (2008).
- [9] S. Giorgini, L.P. Pitaevskii, and S. Stringari, *Phys. Rev. A* **54**, R4633 (1996).
- [10] J.R. Ensher *et al.*, *Phys. Rev. Lett.* **77**, 4984 (1996).
- [11] F. Gerbier *et al.*, *Phys. Rev. Lett.* **92**, 030405 (2004).
- [12] R. Meppelink *et al.*, *Phys. Rev. A* **81**, 053632 (2010).
- [13] G. Roati *et al.*, *Phys. Rev. Lett.* **99**, 010403 (2007).
- [14] R.L.D. Campbell *et al.*, *Phys. Rev. A* **82**, 063611 (2010).
- [15] C. Chin, R. Grimm, P. Julienne, and E. Tiesinga, *Rev. Mod. Phys.* **82**, 1225 (2010).
- [16] M. Houbiers, H.T.C. Stoof, and E.A. Cornell, *Phys. Rev. A* **56**, 2041 (1997).
- [17] M. Holzmann, W. Krauth, and M. Naraschewski, *Phys. Rev. A* **59**, 2956 (1999).
- [18] P. Arnold and B. Tomášik, *Phys. Rev. A* **64**, 053609 (2001).
- [19] M.J. Davis and P.B. Blakie, *Phys. Rev. Lett.* **96**, 060404 (2006).
- [20] O. Zobay, *Laser Phys.* **19**, 700 (2009).
- [21] M. Zaccanti *et al.*, *Nature Phys.* **5**, 586 (2009).
- [22] N. Tammuz *et al.*, *Phys. Rev. Lett.* **106**, 230401 (2011).
- [23] The shot-to-shot temperature fluctuations near N_c are at the 1% level. The slow T drift over the whole series is $<10\%$ and analytically corrected for as described in [22].
- [24] We determine small N_0 's by a direct summation over the density distribution in the central part of the image, after subtracting a fit to the smooth thermal background. For $N_0 > 2000$ this agrees with a standard Thomas-Fermi fit, but is more reliable for smaller condensates.
- [25] The calibration of the y axis in Fig. 3 is done by ensuring that this fit extrapolates to $\Delta T_c/T_c^0 = 0$ for $a/\lambda_0 \rightarrow 0$. If we instead assume that Eq. (2) is exact for $a/\lambda_0 = 0.005$, our results remain the same within error bars.
- [26] F. Gerbier *et al.*, *Phys. Rev. A* **70**, 013607 (2004).
- [27] C.R. Monroe *et al.*, *Phys. Rev. Lett.* **70**, 414 (1993).
- [28] Following [29], we use $\gamma_{\text{el}} = n(0)v_{\text{th}}\sigma_0/2$, where $n(0) = N\bar{\omega}^3(m/2\pi k_B T)^{3/2}$, $v_{\text{th}} = \sqrt{8k_B T/\pi m}$, and $\sigma_0 = 8\pi a^2$.
- [29] H. Wu, E. Arimondo, and C.J. Foot, *Phys. Rev. A* **56**, 560 (1997).